INTERNATIONAL SOCIETY FOR
SOIL MECHANICS AND
GEOTECHNICAL ENGINEERING

SIMSG ISSMGE

This paper was downloaded from the Online Library of the International Society for Soil Mechanics and Geotechnical Engineering (ISSMGE). The library is available here:

https://www.issmge.org/publications/online-library

This is an open-access database that archives thousands of papers published under the Auspices of the ISSMGE and maintained by the Innovation and Development Committee of ISSMGE.

The paper was published in the proceedings of the 10th International Conference on Physical Modelling in Geotechnics and was edited by Moonkyung Chung, Sung-Ryul Kim, Nam-Ryong Kim, Tae-Hyuk Kwon, Heon-Joon Park, Seong-Bae Jo and Jae-Hyun Kim. The conference was held in Daejeon, South Korea from September 19th to September 23rd 2022.

Physical Modelling in Geotechnics
© 2022 KOREAN GEOTECHNICAL SOCIETY (KGS), Seoul, Korea, ISBN 978-89-952197-7-5

Centrifuge tests on the scale effect on the hydraulic gradient of backward erosion piping

M. Okamura, Y. Tsuyuguchi & K. Ono
Graduate School of Science and Engineering, Ehime University, Matsuyama, Japan

ABSTRACT: Hydraulic gradients that cause backward erosion piping are influenced by centrifugal acceleration and this "g scale effect" is a concern for physical modelling. This paper presents the results of 1g and centrifuge tests on backward erosion piping to facilitate better understanding of the mechanism of the g scale effect. The 3D profile of the pipe and flow rate of water in the pipe were observed through a transparent model levee. The normalised bed shear stress (θ_c) estimated for the model pipes were found to be consistent with the Shields diagram. The "g scale effect" on the hydraulic gradient for extending pipes observed in this study is partly explained by the change in θ_c with the particle Reynolds number.

Keywords: backward erosion piping, river levee, centrifuge test, Shields number.

1 INTRODUCTION

River levees sometimes breach during flooding in the mechanism of backward erosion piping. Backward erosion piping is an important failure mechanism for less permeable river levees founded on sandy aquifers. The piping initiates in concentrated leaks at the downstream soil surface when the hydraulic forces imposed by seepage exceed the capacity of the soil to resist them. The erosion process continues, and the pipe extends in the sand layer towards the upstream direction. Eventually, the pipe forms a direct connection between upstream and downstream, which accelerates erosion resulting in levee collapse and breach.

Backward erosion piping is a complex mechanism of coupled water flow and sand particle transport. The current state of knowledge is largely empirical despite considerable research efforts. Physical modelling has played a major role in investigating this complex problem. However, various experiments have confirmed (e.g. van Beek et al.2015) that the hydraulic gradient for generating pipe decreases with increasing seepage length. Scaled model tests provide the hydraulic gradient on the unsafe side. The physics underlying this scale effect is still unclear.

Full-scale physical modelling, especially for the investigation of failures, has limited practical use owing to cost and safety. Centrifuge tests on backward erosion piping have been conducted in recent years and revealed that the hydraulic gradient for generating backward erosion piping decreased with increasing centrifugal acceleration. This "g scale effect" resembles the effect of the seepage length (van Beek et al. 2010; Koito et al. 2016). However, centrifuge modelling also has concerns with appropriate scale factors. The identification of the mechanism of "g scale effects" is an important issue.

This paper presents the results of 1g and centrifuge tests on backward erosion piping to provide a better understanding of the mechanism. This study focussed on the condition of extending the pipe, rather than initiation. An attempt was made to explain the scale effect of centrifugal acceleration on the hydraulic gradient using a non-dimensional number for initiating sand transport in the pipes.

2 INTERACTION BETWEEN FLOW AND SAND TRANSPORTATION IN A PIPE

For a horizontal pipe in a sand bed, sand particles on the bottom of the pipe move when the drag force of the water flow exceeds the frictional resistance of the sand particles. The triggering of sand transportation in the form of rolling and sliding on the bed has been expressed by the Shields number θ_c which is a function of the particle Reynolds number, R_{ep}, and validated by many experiments (e.g. Iwagaki, 1956).

$$\text{Shields number: } \theta_c = \frac{{u_{*c}}^2}{G_s' g d} \tag{1}$$

$$\text{Particle Reynolds number: } R_{ep} = \frac{u_{*c} d}{\nu} \tag{2}$$

where u_{*c}, G_s', d, ν and g are the critical shear velocity at which transportation of sand particles on the bed begins, the submerged specific gravity of sand, the diameter of the sand particle, the kinematic viscosity of water, and the gravitational acceleration, respectively.

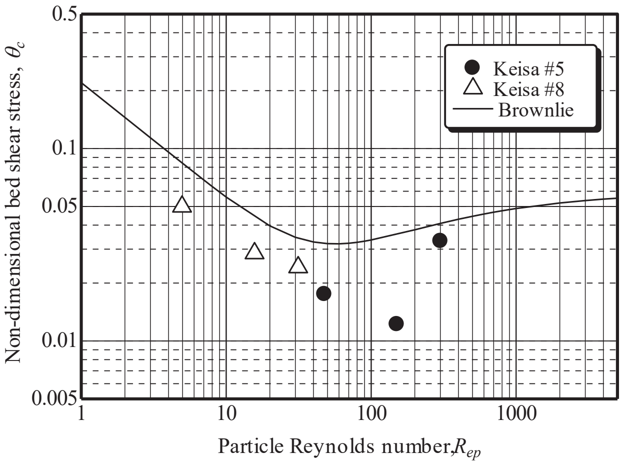

Fig. 1. Shields diagram.

Brownlie (1981) proposed the following equations as explicit forms, as shown in Fig. 1.

$$\theta_c = 0.22 R_{ep}^{\ 0.6} + 0.06 \times 10^{-7.7 R_{ep}^{\ 0.6}} \quad (3)$$

$$R_{ep} = \frac{(G_s' \ g)^{0.5} d^{1.5}}{\upsilon} \quad (4)$$

Iwagaki (1956) proposed a simple equation for obtaining the critical shear velocity u_{*c} directly from the sand particle diameter. The shear velocity u_* is given by,

$$u_* = \sqrt{\frac{f}{8}} u_0 \quad (5)$$

where u_0 and f represent the average flow rate and the dimensionless friction factor in the Darcy-Weisbach equation, respectively. The value of f depends on the Reynolds number of the flow, R_e (= Du_0/ν), and the relative roughness of the pipe d/D, where D is the pipe diameter. For a laminar flow in a pipe.

$$f = 64/R_e \quad (6)$$

While for turbulent flow, f for a rough pipe surface can be approximated using the Colebrook equation.

$$\frac{1}{\sqrt{f}} = -2\log_{10}\frac{2d}{D} + 1.74 \quad (7)$$

3 CENTRIFUGE TESTS

The centrifuge tests in this study aimed at exploring the physics underlying the *g* scale effect. To discuss the applicability of the Shields diagram, the flow rate in the pipe and the 3D profile of pile were measured. Both the grain size of the sand and centrifugal acceleration were varied to test the Shields number over a wide range of R_{ep} (Eq. 4).

3.1 Model preparation

Figure 2 shows the model configuration consisting of a uniform medium dense sand bed and a model levee resting on it. Two sands, Keisa #5 and Keisa #8, were used in the tests, and their physical properties are summarised in Table 1. The model levee was transparent so that a pipe developing on the surface of the sand bed was visibly observed. The dry sands were air-pruviated in the model container at a target relative density of 60%. The model levee was fabricated by gluing acrylic plates. A part of the base plate was cut and filled with UV resin in which a small hole is easily drilled using a hand auger without disturbing the sand and pipe below. A high-speed camera was set on the levee to closely observe the movement of sand in a pipe through the base plate. A laser profiler capable of moving on liner ways was mounted to obtain a 3D profile of the surface of the sand, and hence, the pipe.

Table 1. Physical properties of sand

Sand	Specific gravity, Gs	Mean grain size, D_{50} (mm)	Uniformity Coef. D_{60}/D_{10}	Void ratios, e_{max} / e_{min}	Permeability coef. K (m/s)
Keisa #5	2.64	0.52	1.66	0.73/0.51	5.7×10^{-4}
Keisa #8	2.64	0.12	1.81	1.43/0.75	3.7×10^{-5}

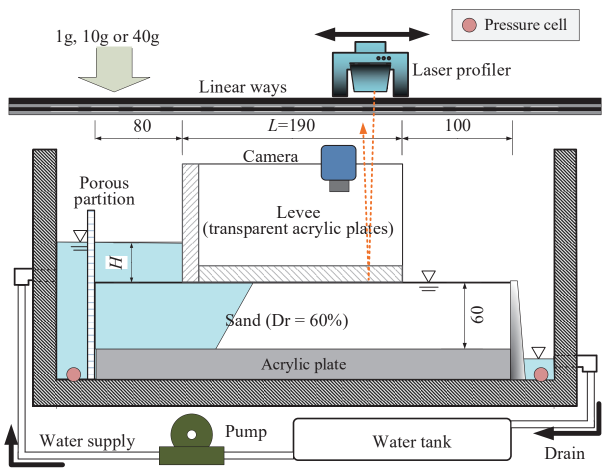

Fig. 2. Model setup; all dimensions are in mm.

3.2 Test procedure

The model was mounted on a geotechnical centrifuge at the Ehime University and spun up to 40g. Water was supplied by the pump to saturate the sand bed prior to the flooding events. The upstream water head was controlled while the water table was kept constant to the surface of the sand bed on the downstream side.

The water head was increased stepwise until sand ejecta appeared at the levee toe, and pipe began to develop. The head was kept constant for a while and decreased to $H = 0$ when the length of the pipe reached approximately 80 mm and the centrifuge was halted. A small hole was carefully drilled immediately above the pipe tip through the UV resin and filled with dye and tracers. The upstream head was gradually increased until the sand in the pipe moved, followed by immediate lowering of the water head to avoid further

© 2022 KOREAN GEOTECHNICAL SOCIETY (KGS), Seoul, Korea, ISBN 978-89-952197-7-5

sand transportation and possible changes in pipe geometry. The dye and tracers flowing in the pipe from the hole were recorded using the high-speed camera. This procedure for identifying the critical head, H_l, at which sand particles in the pipes began to move and the flow rate in the pipe was repeated at 10g and 40g. Finally, water was drained, the model levee was removed and the digital elevation model (DEM) of the pipe was obtained using the laser profiler.

4 RESULTS AND DISCUSSIONS

The time histories of the head and evolution of the pile for the test on Keisa #5 sand bed are shown in Fig.3, where pipe length (l) is the distance between the levee toe and the tip of the pipe. The onset of piping was detected at 40g in the form of sand ejecta from the toe when H = 52 mm. The pipe rapidly developed upstream and reached l = 82mm. At 1g, a small hole of 2 mm diameter was drilled and filled with dye and tracers. The head gradually increased, and the sand in the pipe began to move at H_l = 63 mm. The centrifuge was spun up and the procedure to identify the critical hydraulic gradient was repeated. The observed H_l were 40mm and 32mm at 10g and 40g, respectively. The observed head needed to move sand in the pipe with l = 82mm was lower than that required to initiate the pipe and decreased with increasing centrifugal acceleration. In the preliminary tests, it was observed that after sand started to move at a limited location in the pipe when H_l was reached, a small increase in H of 5 mm was sufficient to move sand almost everywhere over the length of the pipe. This suggests that sand particles everywhere in a pipe are at a critical condition when the head is H_l. The drag force of the water flow was in equilibrium with maximum frictional resistance of the sand particles.

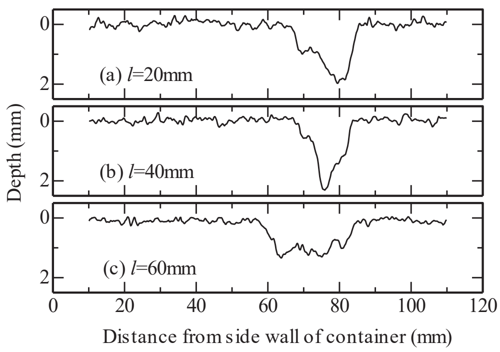

Fig. 3. Time history of water level and pipe length.

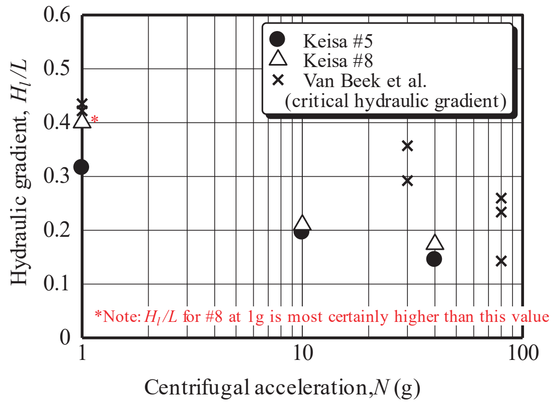

Fig. 4. Relationship between Hydraulic gradient (H_l/L) and centrifugal acceleration.

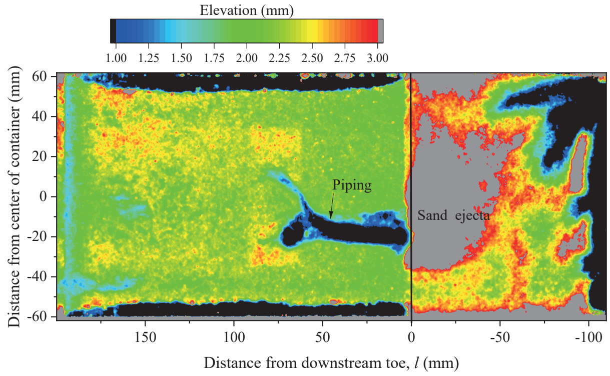

Fig. 5. Elevation of sand surface after the test for Keisa #5.

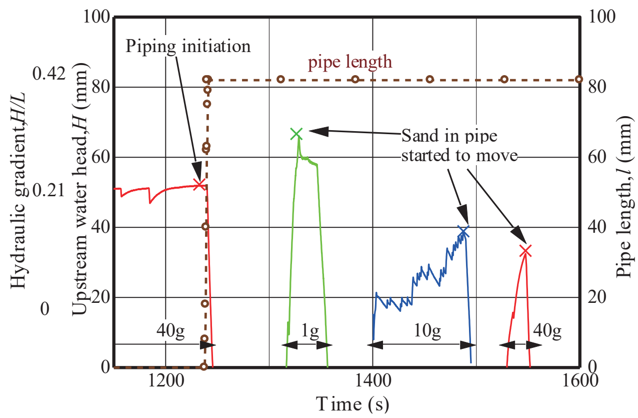

Fig. 6. Cross sections of pipe (Keisa #5).

Fig.4 shows the hydraulic gradient, H_l/L, for the l approximately 80 mm. The hydraulic gradient decreases significantly as increasing in the centrifugal acceleration. Note that the sand in the pipe did not move at H/L= 0.4 in the Keisa #8 test at 1g and the head could not be increased further due to mechanical trouble of the pump. A similar decrease in the hydraulic gradient was reported by van Beek et al. (2010). The elevation of the sand surface, which was measured with the laser profiler after the tests is presented in Fig.5 for the Keisa #5 test. A piping hole from the levee toe extended 82 mm towards the upstream side, which branched at l= 70 mm from the toe. The transported sand from the pipe was stacked in the form of a sand volcano on the downstream surface. The cross sections of the surface below the levee at l = 20, 40 and 60 mm are shown in Fig. 6. The cross sections of the piping channel were typically 2 mm deep and 30 mm wide. The pipe cross-sections are converted to circular pipes with equivalent diameter D_e, as shown in Fig. 7,

$$D_e = 4A\,/\,P \tag{8}$$

where, A and P are the cross-sectional are and wetted perimeter of the pipe, respectively. D_e is almost constant over the length of the pipe for Keisa #8, while D_e is smaller near the pipe tip for Keisa #5.

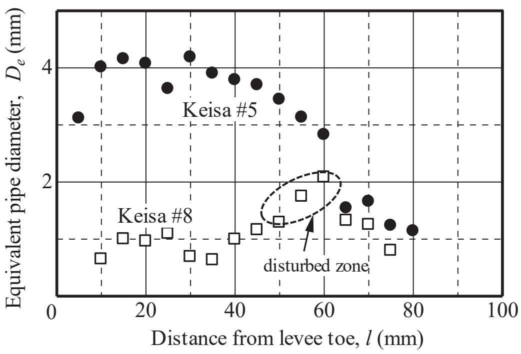

Fig. 7. Variation in diameter of equivalent circular pipe.

The average flow velocity, u_0, when the sand particles started to move ($H = H_l$) is shown in Fig. 8, along with the Reynolds number of the pipe, R_e. Velocities were measured for three pipe ranges of l = 0-20 mm (near the exit), 20 – 40 mm (middle) and 40 – 60 mm (near the tip) for Keisa #5 test, and a range of l = 20 – 40 mm (middle) for Keisa #8 test. For Keisa #8, Re was 11 and 221 for 1g and 40g, respectively, confirming laminar flow in the pipe. The flow in the pile for Keisa #5 at 1g is also laminar (Re ranges from 194 to 327), whereas turbulent flow or transitional flow is inferred at 40g. R_e is higher than 3500 in the ranges of l = 0 – 20 mm and l = 20 – 40 mm, and 2230 in the range near the tip (l = 40 – 60 mm).

The relationship between the Shields number and particle Reynolds number is plotted in Fig. 1 The values of θ_c obtained from the tests are consistent with theoretical values (Shields and Iwagaki); θ_c decreases with increasing R_{ep} for the range of R_{ep} < 48 and increases for R_{ep}>48. For Keisa #5, θ_c near the tip was significantly lower, possible owing to the f value used to evaluate θ_c (Eqs 1 and 5). The f value for the transient flow is highly uncertain and Eq. (6) was tentatively used in this study to provide an estimate close to the lower limit of the f value. Except for this point in the figure, the g scale effect on H_l/L can be well explained by the change in θ_c with R_{ep} and the flow regime. For laminar flow, H_l/L is proportional to θ_c, which is true for Keisa #8. For Keisa #5, θ_c increases with centrifugal acceleration, thus R_{ce}, f increases when the flow regime changes from laminar to turbulent, as indicated by Eqs. (6) and (7). It is to be noted that θ_c derived from the tests is smaller than the theoretical value possibly because of upward water flow at the bottom of pipe, which decreases the submerged weight of sand particles on the bottom of the pipe, is not considered in the theoretical θ_c.

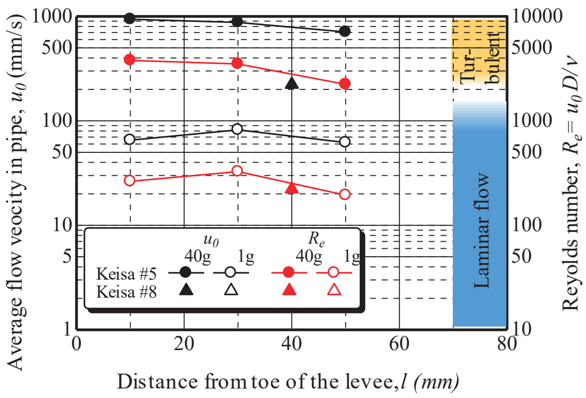

Fig. 8. Flow velocity in the pipes and Reynolds number.

5 CONCLUSIONS

This paper describes 1g and centrifuge tests on backward erosion piping. The hydraulic gradient to extend the pipes decreases with increasing centrifugal acceleration. The 3D profile of pipes and the flow rate of water in the pipes elucidate the flow regime in the pipe. The flow in the pipe for coarse sand (Keisa #5) at 40g was determined to be turbulent. The normalized bed shear stress (θ_c) evaluated for the model pipes is consistent with the Shields diagram. The “g scale effect” on the hydraulic gradient for extending pipes is explained by the change in θ_c with R_{ep}.

ACKNOWLEDGEMENTS

The present research was supported by JSPS KAKENHI (Grant Number 19H00786).

REFERENCES

Brownlie, W.R. 1981. Prediction of flow depth and sediment discharge in open channels, Report No. KH-R-43A, California Institute of Technology.

Iwagaki, Y. 1956. Hydrodynamical study on critical tractive force. *Trans JSCE* No. 41: 1-21. (in Japanese)

Koito, N., Horikoshi, K. & Takahashi, A. 2016.“Physical modelling of backward erosion piping in foundation beneath levee. *Proc. 8th Int. Conf. on Scour and Erosion*: 445–451.

Van Beek V.M., Bezuijen A. & Zwanenburg C. 2010. Piping: Centrifuge experiments on scaling effects and levee stability. *Proc. 7th International Conference on Physical Modelling in Geotechnics*: 183-189.

Van Beek V.M., Van Essen H.M., Vandenboer K, & Bezuijen A. 2015. Developments in modelling of backward erosion piping. Géotechnique 65(9), 740–7